

Energy transfer processes in electron beam excited mixtures of laser dye vapors with rare gases

G. Marowsky

Max-Planck Institut für Biophysikalische Chemie, D 3400 Göttingen, Federal Republic of Germany

R. Cordray, F. Tittel, and B. Wilson

Electrical Engineering Department, Rice University, Houston, Texas 77001

J. W. Keto

Physics Department, University of Texas at Austin, Austin, Texas 78712

(Received 26 May 1977)

The energy transfer mechanisms for electron beam excited N-92 dye vapor in various buffer gas mixtures have been examined. Optimum conditions for achieving intense dye vapor fluorescence with short duration electron pulse excitation are reported.

INTRODUCTION

Direct electrical excitation of dye vapor lasers has received considerable attention in recent years.^{1,2} Electrical excitation offers the possibilities of overcoming the inherent limitations in efficiency for optically pumped dye lasers, extending the present uv wavelength limit of about 320 nm to shorter wavelengths, and scaling to high power laser systems. In this paper we report results of a study to identify the optimum energy transfer conditions which produce efficient fluorescence yields for electron beam excited high pressure buffer gas-dye vapor mixtures. These measurements were made in order to determine the feasibility of achieving laser action in an electron beam excited dye vapor.

The xanthene dye N-92 was used in these studies since in our previous work³ this dye was found to produce intense fluorescence when buffered. The electron beam excited fluorescence spectrum of this dye and its chemical structure formula are shown in Fig. 1. The fluorescence excited by energy transfer from single and binary buffer gas mixtures has been investigated. This study has focussed on high pressure xenon, argon, and argon mixtures as buffer gases. The dye N-92 appears to be an especially attractive candidate for studying the energy transfer processes between xenon and the dye vapor because of their nearly coincidental excited state energy levels. Fig. 2 depicts schematically the basic mechanism. The electron beam energy is first stored in the dense buffer gas and subsequently transferred to the dye vapor. The left-hand side shows the energy level diagram of xenon⁴ with xenon metastables indicated by D^{**} and xenon excimers indicated by D^* . Energy transfer from both states may populate the second electronically excited singlet state S_2 of the dye N-92, followed by a radiationless transition to S_1 and a final deactivation to S_0 accompanied by the desired dye fluorescence.

There are three basic processes by which a buffer gas can contribute to efficient transfer of energy to a radiating dye system: (i) radiative energy transfer from the electron-beam excited buffer gas; (ii) collisional energy transfer; and (iii) breakdown of the buffer gas which provides high densities of low energy electrons for electron impact excitation of the dye. We have found that

collisional excitation from the metastable states of the rare gas buffer atoms and molecules and electron impact excitation appear to be the dominant processes for coupling electron beam energy to the dye vapor. By optimizing the buffer gas composition, the total pressure, and the electron beam deposition it is possible to enhance the fluorescence yields of excited state populations of buffer gas-dye vapor mixtures. Due to the complexity of these mixtures under high levels of excitation, no quantitative measurements on kinetic parameters such as relevant rate constants and collisional and radiative lifetimes have been obtained as yet.

EXPERIMENT

The experimental configuration consisted of a heated stainless steel dye vapor laser cell, mounted directly to a Physics International Pulserad 110 electron beam accelerator. The experimental arrangement is similar to the one described in Ref. 3. Several improvements were made to the diode design and transverse pumping geometry used in our previous work. In an effort to obtain a more uniform electron current distribution across the excitation region, the cathode was redesigned so that it was flat faced rather than wedge shaped. A bronze grid, slightly convex towards the cathode, served as the anode. This grid provided an improved electric field profile and better beam focussing through the sup-

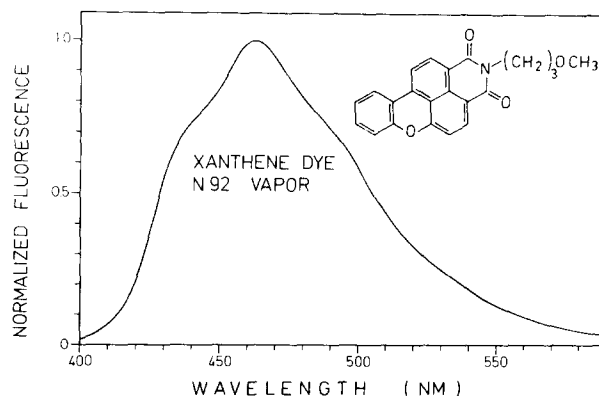


FIG. 1. Electron beam excited fluorescence spectrum of the xanthene dye N-92 together with its chemical structure.

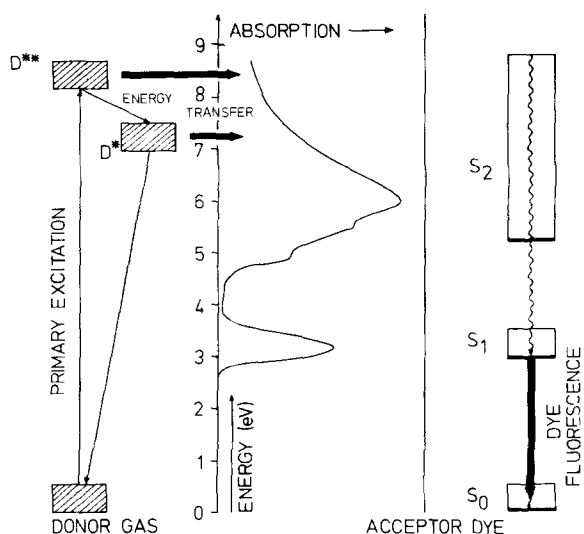


FIG. 2. Schematic diagram of the energy transfer mechanisms from excited xenon buffer gas to the N-92 dye vapor, showing the electronic structure and absorption spectrum.

ported anode foil into the cell. A 3 mil thick titanium foil was used which had a much longer lifetime than the 1 mil thick Havar foil that was used previously. The anode foil was separated from the anode grid by a $1\frac{1}{2}$ cm drift space.

The electron beam distribution was determined using a thermally sensitive film. It was found to be essentially uniform over a transverse area of 8 by 1 cm. The electron energy and current flux as a function of depth into various buffer gases were measured using a Faraday cup and a calorimeter which could be moved to various distances from the anode foil. Both energy and current dropped by a factor of two within the 4 cm distance from the anode foil to the optical axis. For a gas pressure of 3 atm, and with a 7.5 cm long cathode and an 0.8 MeV diode voltage, an energy density of 2 J/cm² and a current density of 80 A/cm² were measured.

The electron beam excited fluorescence intensity and temporal behavior were monitored by a fast planar photodiode (ITT FW114). The spectral characteristics were determined using a grating spectrograph with a 1 nm resolution over the range 250–700 nm, using Polaroid type 410 (ASA 10 000) film as the recording material. The spectral bandwidth of the N-92 fluorescence was typically 80 nm. A comparison of the fluorescence spectrum of electron irradiated and nonirradiated N-92 in a cyclohexane solution showed that the dye suffered little if any degradation after heating and multiple exposures to energetic electron bombardment in a high pressure buffer gas environment.

Measurements of the fluorescence of a 10:1 commercially prepared mixture of Ar–N₂ at 3 atm pressure were used for calibration. With an 8 cm long optical cavity mounted inside the dye cell, this mixture produced intense laser emission of 7 ns duration and peak powers of about 100 kW from the 357.7 and 380.5 nm lines of nitrogen⁵ when pumped by a 0.8 MeV, 15 kA, 10 ns duration electron beam. The optical resonator consisted of a 1 m radius of curvature mirror (with a re-

flectivity greater than 99.6%) and a flat mirror (reflectivity of about 95%) which was used as the output coupler. All dye vapor fluorescence data were compared to the fluorescence of this premixed Ar–N₂ mixture to get an estimate of the potential lasing ability of the electron beam excited dye vapor.

RESULTS

A. Xenon-N-92 mixtures

Among the rare gases, xenon should be superior as a buffer gas for dye vapors because of its greater stopping power.⁶ For the purpose of optimization of the dye fluorescence we studied the influence of the buffer gas over a wide range of both dye vapor pressure and buffer gas pressure. The dependence of the optimum buffer pressure on the dye concentration provides us with valuable hints on the mechanisms for energy transfer. Of special interest is charge transfer from Xe^* and excitation transfer from the electron beam excited Xe^* atoms and the Xe_2^* molecules. Due to the three-body processes involved in the formation of Xe_2^* molecules, all reactions involving Xe_2 molecules should show a strong pressure dependence. Our previous studies^{3,7} established a linear dependence of the time-integrated electron beam excited dye fluorescence in the presence of up to 2 atm of xenon buffer gas with increasing dye density for the dyes *p*-terphenyl, POPOP, and N-92. In addition to the xenon excimer transition centered at 172 nm,⁸ the electron excitation of the high pressure xenon buffer gas alone produced a broad excitation continuum ranging from 300 to 600 nm, primarily due to the admixture of small amounts of impurities such as N₂, H₂O, and other gases. The influence of small amounts of krypton has been discussed.^{9(a)}

If radiative transfer were the predominant form of energy transfer, the extinction of fluorescence from electronically excited xenon states would be governed by optical absorption by the dye. The amount of radiative transfer was determined by experimental observation of the 172 nm band (observed in second order) and the 300–600 nm visible continuum^{9(b)} as a function of dye vapor pressure. For a semiquantitative comparison, a rectangular active geometry as shown in Fig. 3 may be considered. If variations of the pump intensity trans-

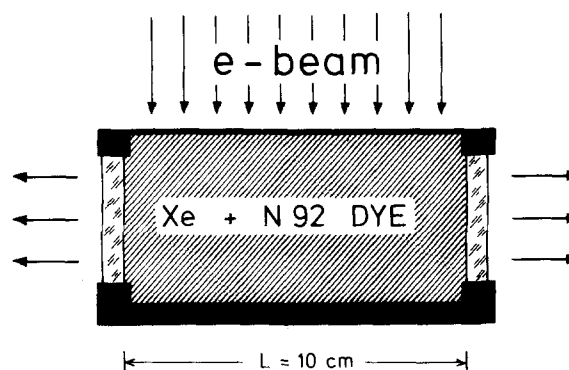


FIG. 3. Electron beam excited xenon buffer gas in the dye vapor reaction cell.

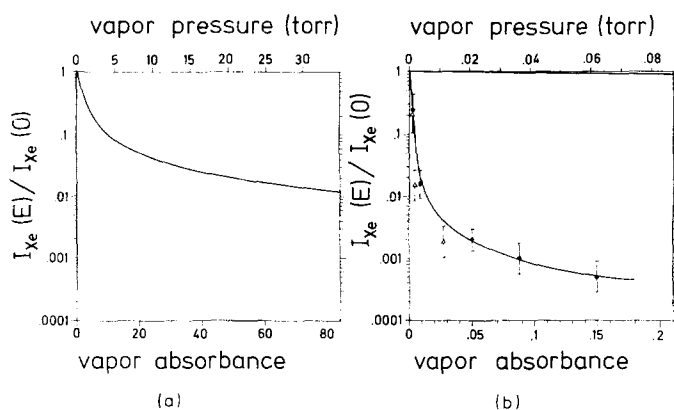


FIG. 4. Normalized intensity of xenon fluorescence expected from dye absorption vs dye vapor pressure (a), and measured intensity of xenon fluorescence at 170 nm (circles) and at 400 nm (triangles) vs dye vapor pressure (b).

verse to the optical axis are neglected, the expected absorption of electron beam excited xenon fluorescence can be estimated by a straightforward integration of Beer's law along the optical axis. Figure 4(a) shows the dependence of the xenon fluorescence emerging from both windows of the reaction cell on dye vapor pressure or vapor absorbance. The fluorescence intensity has been normalized against the fluorescence in the absence of the dye vapor [$I_{Xe}(E=0)$]. The vapor pressure data and the vapor extinction coefficient have been taken from Ref. 10. It is apparent from Fig. 4(a) that due to the large optical path length the dye vapor cannot be considered as optically thin. However, as shown in Fig. 4(b), the xenon fluorescence is quenched strongly even at extremely low dye vapor concentrations. The xenon fluorescence output, as monitored by the extinction of the 172 nm band [circles in Fig. 4(b)], decreases far more rapidly than calculated for pure radiative energy transfer [note the portion of the extinction curve at the top of Fig. 4(b)]. Therefore, radiative energy transfer does not play a dominant role for dye vapor pressures from 10 to 50 torr. As shown by the triangular symbols in Fig. 4(b), the visible part of the xenon excitation spectrum, as monitored at 400 nm, decreases even faster with dye vapor pressures as low as 1/100 of one torr. Various tests indicated that no dye decomposition occurred as a result of well buffered dye vapor mixtures as shown by identical fluorescence and absorption spectra of both, radiated and nonradiated POPOP samples.

In Fig. 5 are shown two typical oscillograms depicting the temporal behavior of the dye fluorescence at a constant dye pressure of 0.5 torr. Figure 5(a) was taken at 1.5 atm xenon gas pressure, and Fig. 5(b) at 3 atm pressure. Two distinct dye fluorescence peaks are apparent with a temporal separation of about 30 ns for Fig. 5(a). These two peaks show a different evolution as the buffer gas pressure is increased. When the buffer gas pressure is increased by a factor of two, the first peak increased less than twice, whereas the second peak increases more than twice. This time and intensity behavior may be explained by the formation of xenon excimers, which are created when an excited xenon atom collides with a ground state xenon atom. We

attribute the primary peak with a rise and fall time comparable to the behavior of the electron beam pulse to collisional interaction between excited metastable xenon and dye molecules. The secondary peak, with a relatively slow rise and decay time of about 30 ns, can be attributed to fluorescence from dye molecules excited by collisions with Xe_2^* molecules. We ascertained that both peaks were indeed due to dye fluorescence, and not xenon fluorescence, by placing a short wavelength cutoff filter in front of the photodiode. The response was unaffected. Since the lifetimes for $Xe_2^*(0_u^+)$ and $Xe_2^*(1_u)$ are 6 and 100 ns, respectively, the effective decay time of both these states in the presence of high electron densities is of the order of 20–40 ns.¹¹ If we take into account the known rate constant $k \approx 10^{-31} \text{ cm}^6 \text{ s}^{-1}$ for the production of $Xe_2^*(0_u^+ \text{ and } 1_u)$,¹² a temporal separation between the peaks of about 30 ns is obtained at a xenon pressure of 1 atm which is consistent with our observations. The secondary peak shifts towards earlier time with increasing gas pressure. Lines characteristic of the Xe_2^* could also be detected as a second order diffraction with the spectrograph. The observed temporal behavior was seen with different dyes, and did not depend upon dye concentration. Therefore, we assume that this secondary peak cannot be explained in terms of delayed fluorescence due to triplet effects.¹³ It is important to note that although most of the integrated intensity is associated with the second peak, its risetime at the low total pressure of these experiments is too slow for efficient laser pumping of dyes due to triplet loss mechanisms. The integrated intensity of the second peak increases linearly with both xenon and dye-vapor pressure. In Fig. 6 we show the first peak intensity as a function of xenon pressure at dye densities ranging from 0.04 to 20 torr. The dye fluorescence peak associated with the leading component always appears at xenon pressures of 1.5 to 2.0 atm, independent of the dye-vapor pressure, suggesting that the peak dye intensity cannot be attributed to excitation transfer from Xe^* alone. Furthermore, we find a relatively fast saturation of peak dye fluorescence with increasing dye vapor pressure while the time integrated fluorescence increases linearly with dye vapor pressure (Fig. 5 in Ref. 3).

We may conclude from these measurements that in order to utilize the energy transferred to the dye from

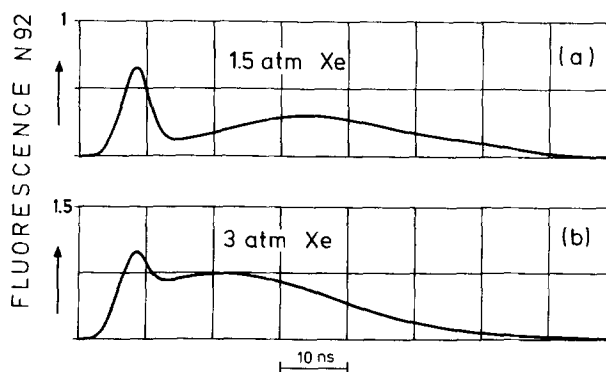


FIG. 5. N-92 fluorescence (relative units) at two different xenon buffer gas pressures (retraced oscillograms).

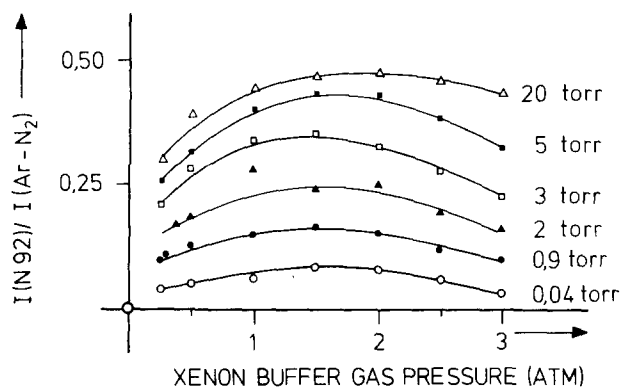


FIG. 6. Normalized N-92 fluorescence intensity (fast peak) versus xenon buffer gas pressure for various dye vapor pressures.

excimers formed at higher xenon pressures, sufficient pressure (>7 atm) is required in order to shorten molecular production times to the order of the dye fluorescence lifetime. Such pressures will require redesigning of the stainless steel cell for higher temperature and pressures. However, the heavy atom effect might interfere with these efforts for optimization of the buffer gas system.¹⁴ It is well known that xenon is particularly effective in this respect at high pressures. It can enhance the intersystem crossing rate in the dye molecules, thus increasing the triplet population and finally decreasing the fluorescence intensity. This may explain part of the previously observed saturation of the time integrated fluorescence at higher xenon pressures (Fig. 6 of Ref. 3).

B. Argon-N-92 mixtures

The most promising gas system studied was argon in the pressure region 1–7 atm. Although argon has a lower stopping power and a greater energy transfer mismatch than xenon, it has been shown to be very effective in energy transfer both in binary and ternary dye vapor–buffer gas mixtures. The Ar–N₂ laser⁵ and the various electron beam pumped Ar buffered rare gas–halide

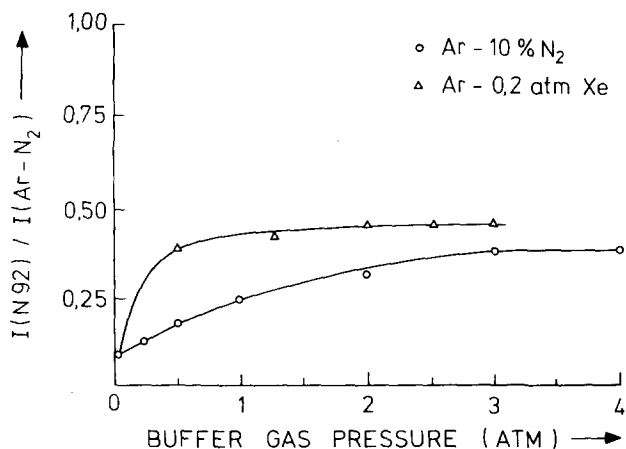


FIG. 7. Normalized N-92 fluorescence at a constant dye vapor pressure of 7 torr with a mixture of Ar–N₂ and argon and 0.2 atm xenon vs total buffer gas pressure.

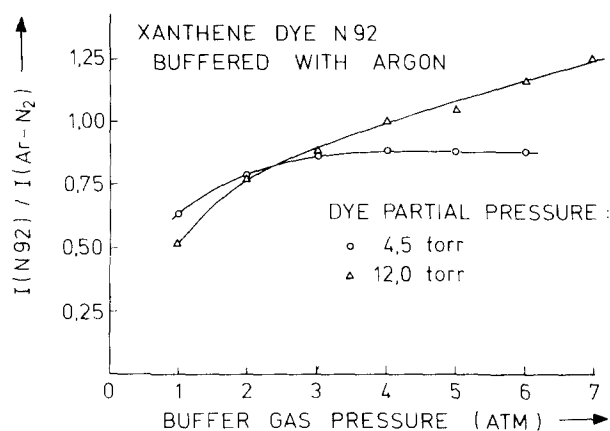


FIG. 8. Normalized N-92 fluorescence versus pure argon buffer gas pressure for two dye vapor pressures.

lasers such as the KrF or XeF lasers^{15,16} demonstrate the good excitation transfer properties of argon. Also, measurements on Ar–POPOP mixtures at 3 atm total pressure by Edelstein *et al.*¹⁷ gave photon yields about four times higher in argon than in xenon.

Ternary mixtures of dye vapor with argon, and either nitrogen or xenon, as well as with pure argon were investigated. The fluorescence intensity of N-92, with buffer gas mixtures of argon with 10% nitrogen, and argon with the addition of a small amount of xenon (0.2 atm) is shown in Fig. 7. Although the fluorescence from the argon–xenon mixture rose faster initially with increasing gas pressure, both gas systems saturated at a modest level of fluorescence. It should be noted that when the argon–nitrogen gas mixture was used, sharp lines, characteristic of nitrogen emission, were visible on the spectrograph recordings. These lines disappeared at higher dye vapor pressure, indicating the possibility of radiative transfer of energy from the nitrogen to the dye was taking place. Earlier measurements³ determined that the absorption band of N-92 overlaps two of the emission lines of nitrogen.

The greatest fluorescence yield was obtained from a pure argon–N-92 mixture. The fluorescence output from the dye, as a function of buffer gas pressure for two dye vapor concentrations, is shown in Fig. 8. At a relatively low dye concentration (4½ torr), the output saturated for argon pressures greater than 3 atm. At a higher dye concentration (12 torr) the fluorescence output continued to increase with argon pressure up to 7 atm, the limit of the present system. Fluorescence measurements taken at intermediate dye pressures indicate that the buffer gas pressure required for optimization of the dye fluorescence strongly increases with dye vapor pressure. Approximately 10 atm Ar buffer gas pressure are necessary to obtain highest fluorescence from the dye N-92 at 380 °C, the breakdown temperature of its chemical structure.¹⁰

The maximum output which was observed at one of the windows from the cell was 335 W. From an estimate of the total energy radiated by the dye, and the measured electron beam intensity, we have calculated that for every primary electron entering the cell, more than 10³

photons are produced. This strongly suggests that the energy transfer to the dye comes from both, excited metastables and secondary electrons emitted from the buffer gas by impact ionization. This observation is in agreement with electron beam excitation studies of fluorescence from molecular beams of POPOP.¹⁸ Our measured dye output corresponds to a maximum photon yield Φ^{17} of about 8% for Ar-N-92 mixtures at a pressure of 7 atm Ar.

CONCLUSIONS

A detailed study of the influence of various buffer gas mixtures in the electron-beam excited fluorescence of the xanthene dye N-92 in the vapor phase shows that argon is the most effective donor for coupling energy from the electron beam to the dye acceptor in the pressure regime 1–7 atm. Collisional energy transfer and secondary electron impact appear to be the dominant processes in the excitation of the dye vapor. The maximum fluorescence yield from an argon–dye mixture increases with dye concentration. The major limiting factor for obtaining greater dye fluorescence output so far appears to be the pressure and temperature handling capabilities of our present dye cell construction, and not dye decomposition.

The effectiveness of xenon as a buffer gas seems to be hindered at the pressures investigated by the formation of the xenon excimer Xe_2^* . We were able to observe this excimer buildup in both the delayed secondary pulse of the dye output, as well as in the 172 nm continuum characteristic of the excimer as seen in second order on the spectrograph at low dye vapor pressures. The fluorescence time constants and their temporal separation corresponds well to the known characteristics of the excited xenon atoms and excimers. From the various experimental findings we conclude that the delayed formation of the Xe_2^* excimers and the potential triplet effects are the main contributions for the limited pumping efficiency of the xenon–dye mixture. Argon, although it has a somewhat lower effective electron beam stopping power, is not evidently affected by triplet intercrossing effects and therefore acts as a more effective buffer gas system for this dye.

ACKNOWLEDGMENTS

The authors would like to thank V. Arakelyan, T. Bonifield, F. P. Schäfer, and G. K. Walters for many stimulating discussions. The work was in part supported by the Energy Research and Development Administration, the Robert A. Welch Foundation, and the National Science Foundation. A NATO travel grant covered part of the travel expenses. One of us (J. W. K.) would like to acknowledge the support of the Joint Service Electronics Program through AFOSR Contract F-44620-76-0089.

- ¹P. W. Smith, P. F. Liao, and P. J. Maloney, *IEEE J. Quant. Electron.* **QE-12**, 539 (1976).
- ²P. F. Liao, P. W. Smith, and P. J. Maloney, *Opt. Commun.* **17**, 219 (1976).
- ³G. Marowsky, R. Cordray, F. K. Tittel, W. L. Wilson, and J. W. Keto, *Appl. Phys.* **12**, 245 (1977).
- ⁴C. K. Rhodes, *IEEE J. Quant. Electron.* **QE-10**, 153 (1974).
- ⁵S. K. Searles and G. A. Hart, *Appl. Phys. Lett.* **25**, 79 (1974).
- ⁶M. J. Berger, S. M. Seltzer, *Tables of Energy Losses and Ranges of Electrons and Positrons* (NASA, Washington, D. C., Rep. N65-1206).
- ⁷G. Marowsky, F. P. Schäfer, J. W. Keto, and F. K. Tittel, *Appl. Phys.* **9**, 143 (1976).
- ⁸S. C. Wallace and R. W. Dreyfus, *Appl. Phys. Lett.* **25**, 498 (1974).
- ⁹(a) R. E. Gleason, Jr., Thesis (Rice University, Houston, TX, 1976). (b) J. F. Prince and W. W. Robertson, *J. Chem. Phys.* **45**, 2577 (1966); and **46**, 3309 (1967).
- ¹⁰B. Steyer and F. P. Schäfer, *Appl. Phys.* **7**, 113 (1975).
- ¹¹J. W. Keto, R. E. Gleason, Jr., T. D. Bonifield, G. K. Walters, and F. K. Soley, *Chem. Phys. Lett.* **42**, 125 (1976).
- ¹²W. Wieme, *J. Phys. B* **7**, 850 (1974).
- ¹³C. A. Parker, *Photoluminescence of Solutions* (Elsevier, Amsterdam, London, New York, 1968).
- ¹⁴K. H. Drexhage, in *Dye Lasers*, edited by F. P. Schäfer (Springer-Verlag, Berlin, Heidelberg, New York, 1973).
- ¹⁵M. L. Bhaumik, R. S. Bradford, Jr., and E. R. Ault, *Appl. Phys. Lett.* **28**, 23 (1976).
- ¹⁶E. R. Ault, R. S. Bradford, Jr., and M. L. Bhaumik, *Appl. Phys. Lett.* **27**, 413 (1975).
- ¹⁷S. A. Edelstein, H. H. Nakano, T. F. Gallagher, and D. C. Lorents, *Optics Commun.*, **21**, 27 (1977).
- ¹⁸P. W. Smith, *Optica Acta* **23**, 901 (1976).